ADVANCED ENERGY MATERIALS
www.advenergymat.de

Lithium-Ion Textile Batteries with Large Areal Mass Loading

*Liangbing Hu, Fabio La Mantia, Hui Wu, Xing Xie, James McDonough, Mauro Pasta, and Yi Cui**

Li-ion batteries are widely used in current applications such as in cell phones and laptops, and the industry is undergoing rapid expansion. Li-ion batteries are believed to be a major power source for future electrical vehicle applications.[1,2] In a typical Li-ion battery, the electrode materials are electrically contacting the current collector through percolative pathways from conductive additives such as conductive carbons. To increase the total energy stored in a battery, the cells are packed in rolls and stacks and then into modules before final packing in large quantity.[2] There are dead cell components such as separators, current collectors and packing in Li-ion batteries, which will increase the cost and decrease the total energy density. The total mass of both positive and negative electrode accounts for less than 50% of the total weight.[3] Traditionally, electrode materials are loaded on the surface of the metal current collector through roll coating methods. The typical thickness for the battery electrode material is ~ 50 μm with a mass of ~20 mg/cm^2.[4] A higher areal mass loading of battery electrode materials is preferred which will reduce the number of manufacturing steps for achieving the same total energy and also lower the separator costs. However, the traditional architecture of battery electrode materials on flat metal current collectors does not allow for higher mass loadings due to the following major difficulties: (1) Thick electrodes tend to delaminate from the flat current collectors during the high-speed roll-to-roll coating process. (2) The difficulty of electrolyte penetration through a thick electrode which dramatically increases the cell impedance, and, as a consequence, a loss of energy efficiency.

The concept of three dimensional (3D) battery electrodes has been used previously to enhance the energy per footprint area.[5] Here we adapt a 3D porous textile conductor as a replacement for metal current collectors. Previously supercapacitors have been demonstrated based on conductive paper and textile.[6–10] Compared with supercapacitor, Li-ion batteries have much higher energy density per weight. Our study here focuses on the development for Li-ion battery application based on the conductive textiles. The electrode materials are loaded into the 3D pores of conductive textiles through the simple solution based process. We found the stable potential range of such conductive textiles in organic electrolyte, and effectively demonstrated a working Li-ion battery with a mass loading of ~168 mg/cm^2 and a thickness of ~600 μm, which are 8–12 times higher of those on metal collector. Such a thick electrode-current collector architecture shows outstanding performance in capacity retention during cycling and little self-discharge. A control study of electrode materials coated on a flat metal current collector with the same mass loading shows that the film delaminates from the substrate, and there exists a much larger voltage difference between charging and discharging when compared with the 3D electrode-current textile architecture. Impedance studies reveal much smaller device impedance for the 3D electrode-current collector configuration compared to that of flat substrate configuration, which is attributed to the excellent ion transport from the electrolyte to the active material surface and also from the superior charge transport between current collector and electrode materials. Such integrated Li-ion batteries in textiles are also promising for the emerging wearable electronics.[10–14]

Figure 1(a) illustrates the structure of the 3D, porous conductor and its integration with the battery electrode materials. The textile conductor is fabricated using a plain polyester fiber textile and well-dispersed single walled carbon nanotube (CNT) ink in water with the assistant of 1% sodium dodecylbenzenesulfonate (SDBS) to prevent CNT agglomeration.[15] Commercial carbon nanotubes (arc-discharged P3 CNTs, Carbon Solutions, Inc.) are used as received. The metal content of the purified CNT is 5–8% and the average CNT bundle length is approximately 2 μm according to the product description. Note that the conductive textile can also be fabricated with other conductive nanomaterials such as graphenes and multiwalled carbon nanotubes. The conductive textile is rinsed in DI water to remove the excess surfactant until no bubbles are observed. The finished textile is both conductive (sheet resistance of 8 Ohm/sq) and porous, with a thickness of ~2 mm and surface conductivity of ~0.625 S/cm. The conductivity of the CNT coating on polyester fibers is ~1300 S/cm (see Supporting Information). Such porous structure can function effectively as current collector for loading Li-ion battery materials inside. The battery electrode materials will have excellent electrical contact within the conductive polymer fibers. Furthermore, the polyester fibers lead to excellent wetting between the battery electrolyte and the integrated current collector-electrode due to the porosity of polymer fibers.[16,17] After a simple dipping and drying process, a 3D structure with integrated current collectors and battery electrode materials is readily formed. Due to the porous structure, the mass loading per area is high, approximately 168 mg/cm^2 and the thickness is approximately 600 μm. The thickness is much less than the original conductive polyester fiber network due to the textile shrinking caused by the drying process. In contrast, for traditional metal current collectors, the battery electrode material is on the surface. Although roughened metal surfaces are sometimes used, the roughness of metal is much less than

Dr. L. Hu, Dr. F. La Mantia, Dr. H. Wu, X. Xie, J. McDonough, M. Pasta, Prof. Y. Cui
Department of Materials Science and Engineering
Stanford University
Stanford, CA 94305
E-mail: yicui@stanford.edu

DOI: 10.1002/aenm.201100261

ADVANCED ENERGY MATERIALS
www.advenergymat.de

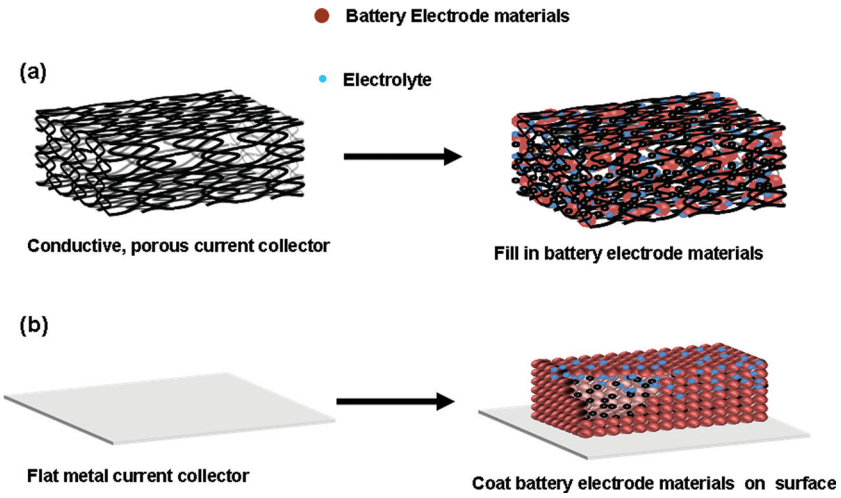

Figure 1. Design and fabrication of 3D porous current collectors filled with the battery electrode material. (a) (left): Highly conductive fibrous network after coating polyester fibers with carbon nanotubes and (right): Porous conductor filled with battery materials, where the conductive polyester fiber network functions as an effective current collector and the organic electrolyte penetrates throughout the entire structure effectively. (b) By comparison, the battery electrode material is coated on the surface of the flat current collector in the traditional architecture.

the thickness of the battery electrode. To avoid delamination during the drying step in high speed processing, the thickness of the battery electrode is typically limited to 50 μm with areal mass of ~20 mg/cm^2.

The 3D morphology of the conductive textile is shown in **Figure 2**(a), where CNTs are conformally coated onto the surface of the polymer fibers. Although the thickness is much larger than a typical Copper (Cu) foil collector (~15–20 μm), the areal weight of the conductive textile is much less than that of the Cu foil (by >60%). The light weight of the conductive textile will contribute to a higher specific energy on the final device. In order to find the operation voltage window of the conductive textile in Li-ion batteries, half cells were made with the conductive textile as the working electrode and a piece of Li-metal as the counter electrode. Coin cells were fabricated using a 1 M solution of $LiPF_6$ in ethylene carbonate (EC)/diethyl carbonate (DEC) (1:1 vol/vol; Ferro) as the electrolyte.

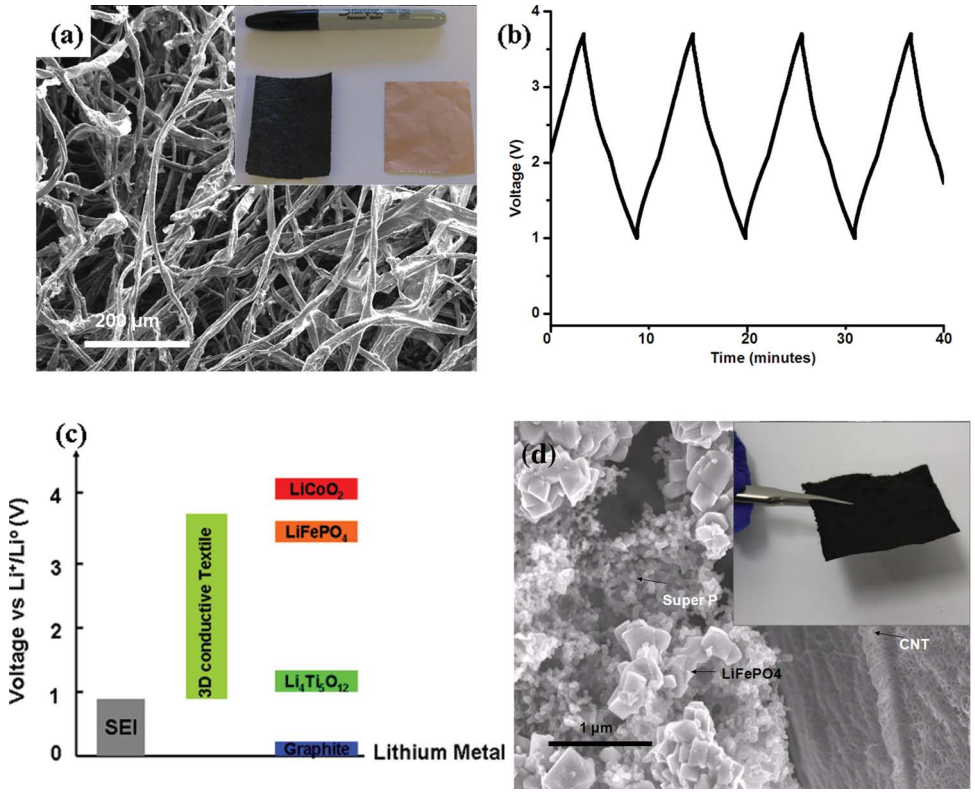

Figure 2. (a) SEM image of conductive textile after CNT coating with porous structure. Inset: A light weight, highly conductive polyester textile with an area of 5 cm^2 (left) and a Cu strip with the same area. The mass of the conductive textile is 30 mg, while the Cu strip with the same area is 50 mg. (b) Charge-discharge profile of conductive textile, which shows good electrochemical stability in the window of 1 V to 3.8 V. (c) Voltage stability window of the 3D conductive textile current collector with widely used electrodes. (d) SEM shows the interface between $LiFePO_4$, conductive additive Super-P, and conductive polyester fibers coated with carbon nanotubes. Inset: A solid textile filled with $LiFePO_4$. The areal mass of $LiFePO_4$ is 168 mg/cm^2 and the thickness is 600 μm.

The cell voltage was monitored as a constant current, 100 μA, was applied. As shown in Figure 2(b) and Supporting Materials, the conductive textile was found to be electrochemically stable in the voltage window of ~0.9 V–3.7 V vs. Li/Li^+ in $LiPF_6$ in EC/DEC electrolyte. Therefore, $Li_4Ti_5O_{12}$, ~1.6 V, was chosen as the anode and $LiFePO_4$, 3.4 V, was chosen as the cathode material in this study (Figure 2(c)). The lower voltage range, ~0.9V, may be due to the large solid-electrolyte-interphase (SEI) formation on the carbon nanotube coating of the 3D textile.[18] The energy textile with the embedded battery electrode material is highly flexible and can be easily cut into various shapes. The interface between the $LiFePO_4$, conductive additive Super-P and CNT-coated polyester fibers is clearly seen in Figure 2(d). As in the typically battery electrode configuration, Super-P carbon is added with a percolative network to electrically connect the battery particles. The charge carriers will transport along the Super-P carbon locally before reaching the CNT-polyester fibers. For comparison, a thick, $Li_4Ti_5O_{12}$ slurry was doctor bladed onto a Cu mesh and dried in a vacuum oven. The films often delaminate from the substrate and had poor final film morphologies. An extremely slow drying process can lead to small areas that can be used for electrochemical testing.

3D textile current collectors not only provide an extremely simple method for increasing the mass loading of the electrode materials, but also lead to much better performance in terms of device overpotential and impedance. Due to the high mass loadings of $Li_4Ti_5O_{12}$ and $LiFePO_4$, larger currents can be applied when Li-metal is used as the counter electrode at a meaningful charge-discharge rate. The large current density will cause instability and fluctuation of potential on Li-metal side, which causes difficulty for voltage measurements using a two-terminal device structure. Therefore, a three-electrode measurement configuration is used. A pouch cell with a reference electrode based on $LiFePO_4$ ($U_{reference}$ = 3.430 V vs. Li/Li^+) was used (**Figure 3**(a)). The counter electrode was a thin metallic lithium film. The reference electrode, $LiFePO_4$, was cycled for 5 cycles and stopped at a 50% state of charge, which provides a flat voltage profile as a reference. This configuration allows for easy observation of the differences in the behavior of the active material with the different current collectors.[19] Note that the reference electrode,

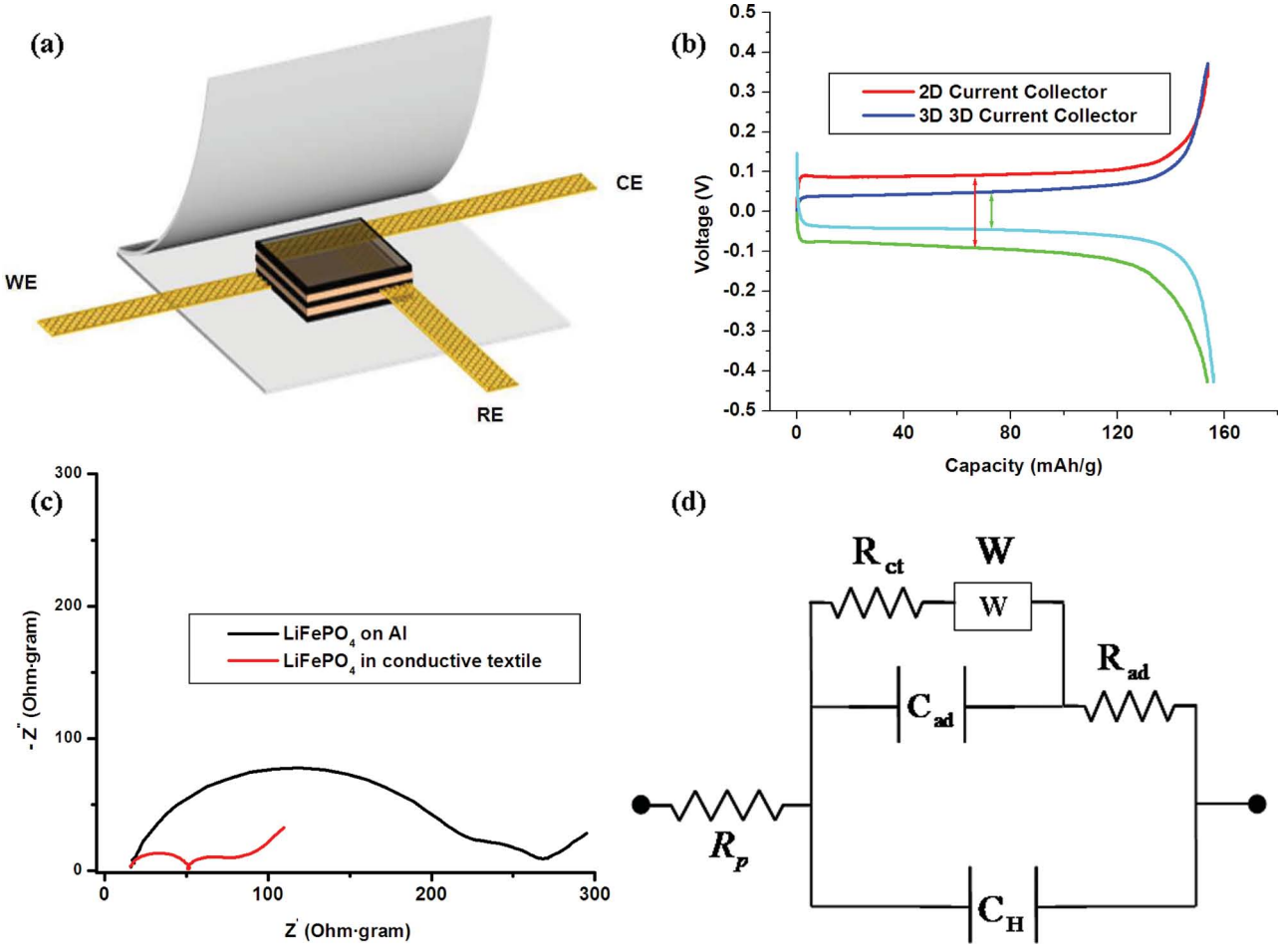

Figure 3. (a) A sketch of a three electrode cell, where CE = counter electrode, WE = working electrode and RE = reference electrode. The cell area is 1 cm by 1.5 cm. (b) Voltage profile of $LiFePO_4$ vs. the reference electrode in the three electrode cell for both 3D and flat architectures, where 3D electrode structures lead to much smaller overpotentials than flat structures. (c) Impedance spectra normalized by the weight of $LiFePO_4$, where the 3D electrode shows much smaller impedance. (d) An equivalent circuit for analyzing impedance data in 3(c).

$LiFePO_4$, was coated onto a Cu mesh to allow efficient Li-ion transport. The 3D textile current collector embedded with 168 mg/cm^2 $LiFePO_4$ was cycled using the device configuration shown in Figure 3(a). The voltage offset in charging and discharging is twice the overpotential of the device, due to the fact that $LiFePO_4$ on Cu mesh was used as the reference electrode. The overpotential for $LiFePO_4$ embedded in the 3D textile electrode is 0.05 V (Figure 3(b)). For comparison, the same test was carried out for $LiFePO_4$ coated on Al foil, where the mass of $LiFePO_4$ is 142 mg/cm^2 with a thickness of ~500 µm (without a mechanical pressing). $LiFePO_4$ did not delaminate from the Al foil in some areas, so pieces from those areas were cut for the test. As shown in Figure 3(b), the overpotential for $LiFePO_4$ on Al is ~0.1 V, which is twice that for $LiFePO_4$ embedded in the 3D textile current collector.

Electrochemical impedance spectroscopy (EIS) was used to identify the differences in the overpotential distribution between the metallic flat current collector and the porous conductive textile. In Figure 3(c) the impedance spectra are reported normalized for the mass loading. EIS meaurements were acquired at OCV (open circuit voltage) in galvanostatic mode (500 µA/g) in the middle of the charge curve, after 5 cycles of full charge and discharge to stabilize the potentials. The general shape of the impedance spectra evidences two semicircles, one in the high frequency and one in the middle frequency region, followed by a linear behavior, with a slope of approximately 45°, which is probably correlated to diffusion limitations.[20] It is interesting to observe that the middle frequency semicircle and the diffusion part of the spectra are similar for both current collectors, while the first semicircle is much smaller for the 3D porous current collector. The impedance spectra were analyzed using the equivalent circuit in Figure 3(d) and the theory of porous electrodes reported in reference.[21] R_{ad} is the adsorption resistance, C_{ad} is the adsorption capacitance, W is the Warburg element, C_H is the capacitance of double layer, R_{ct} is charge transfer resistance and R_p is pore resistance. In **Table 1** the results of the impedance analysis are reported. It can be observed that, while the kinetic parameters are not changing very much with the current collector, the resistance of the electrolyte in the pores, R_p, is decreased of 100 times passing from the aluminum current collector to the CNT-textile current collector. The pore resistance is 768 Ω·mg for 2D current collector and 6.95 Ω·mg for 3D current collector. The model considers that the particles are charged homogeneously in the electrode. It is clear that the main differences between the current collectors consist in the easier access of the ions in the pores. The shape of the semicircle, squashed to the x axis, suggest a strong influence of the porous structure on the overpotential distribution.[22] Given that the active material mass is similar and in the same charge conditions in the two spectra, the difference between the two spectra has to be attributed to the different structure of the current collectors.[22] The 3D textile based electrodes shows much less impedance than Al foil, which explains the overpotential observed in Figure 3(b).

Conductive textiles loaded with the anode material $Li_4Ti_5O_{12}$ were also tested, in which the mass loading was 145 mg/cm^2. The charge and discharge voltage profiles are shown in **Figure 4**(a), The first charge and discharge capacities were 170 mAh/g and 162 mAh/g, respectively, with a Coulombic efficiency of 95%, which is comparable with the performance of the metal substrate with ~20 mg/cm^2 mass loading.[23] The rate is C/10. The $Li_4Ti_5O_{12}$ in the 3D textile electrode with the high mass loading shows excellent cycling performance, with <10% variation of capacity change in 350 cycles (Figure 4(b)). The Coulombic efficiency was typically >99.5%. There is a decrease of capacity around 50 cycles, the reason of which is not clear yet. For practical applications with such 3D structure current collector-electrode structures and high mass loadings, full cells were assembled with $Li_4Ti_5O_{12}$ as the anode and $LiFePO_4$ as the cathode. The Coulombic efficiency of full cells was 87% for the first cycle and typically >99.0% after the first cycle. The full cell shows 88.5% retention of its initial capacity after 30 cycles. Therefore, we successfully demonstrated Li-ion batteries with ~145 mg/cm^2 loading of active materials. Due to the high water moisture absorption ability of textiles, improvement of the drying of the electrodes before battery assembly could further improve the cycling performance. Self-discharge of the full cell was tested after cycling the cells for 10 cycles at C/10. The cell was then charged at C/10, rested for a certain time, and then discharged. The rest time was set at 0.1, 2, 10, 20, 100 and 200 hours. The self-discharge amount was defined as $Q_{loss} = Q_{discharge} - Q_{charge}$, where $Q_{discharge}$- Q_{charge} were charge amounts for the cell before and after resting. Figure S5 shows the voltage profile and the self-discharge for different rest time. 4% self-discharge was observed for our cell after 200 hours, which is comparable with the self-discharge performance of the cells with Al and Cu foil as current collectors fabricated as controlled samples.

In conclusion, we have demonstrated a 3D architecture of integrated battery active materials into porous current collector for Li-ion batteries. The area mass loading is typically ~140–170 mg/cm^2, approximately 7-8 times higher than the traditional Li-ion battery structures. Such current collector-electrode architecture leads to much better performance than that on flat metal substrate with the same mass loading, which is attributed to the lower impedance due to the better electrolyte–active materials or current collector-active material contact. Full cells based on integrated structures show promising results for future applications, which can lead to low cost devices due to the simple fabrication process and reduction in the overall amount of separator material needed in the devices.

Table 1. Impedance analysis of data in Figure 3(c) with a modeling in reference [12].

	C_H F mg^{-1}	R_{ad} Ω mg	C_{ad} F mg^{-1}	R_{ct} Ω mg	W S s$^{-0.5}$ mg^{-1}	R_p Ω mg
2D Current Collector	$1.14 \cdot 10^{-5}$	$6.60 \cdot 10^{+1}$	$9.43 \cdot 10^{-4}$	$2.35 \cdot 10^{+1}$	$1.29 \cdot 10^{-1}$	$7.68 \cdot 10^{+2}$
3D Current Cellector	$1.11 \cdot 10^{-6}$	$2.74 \cdot 10^{+1}$	$1.05 \cdot 10^{-3}$	$2.41 \cdot 10^{+1}$	$7.86 \cdot 10^{-2}$	6.95

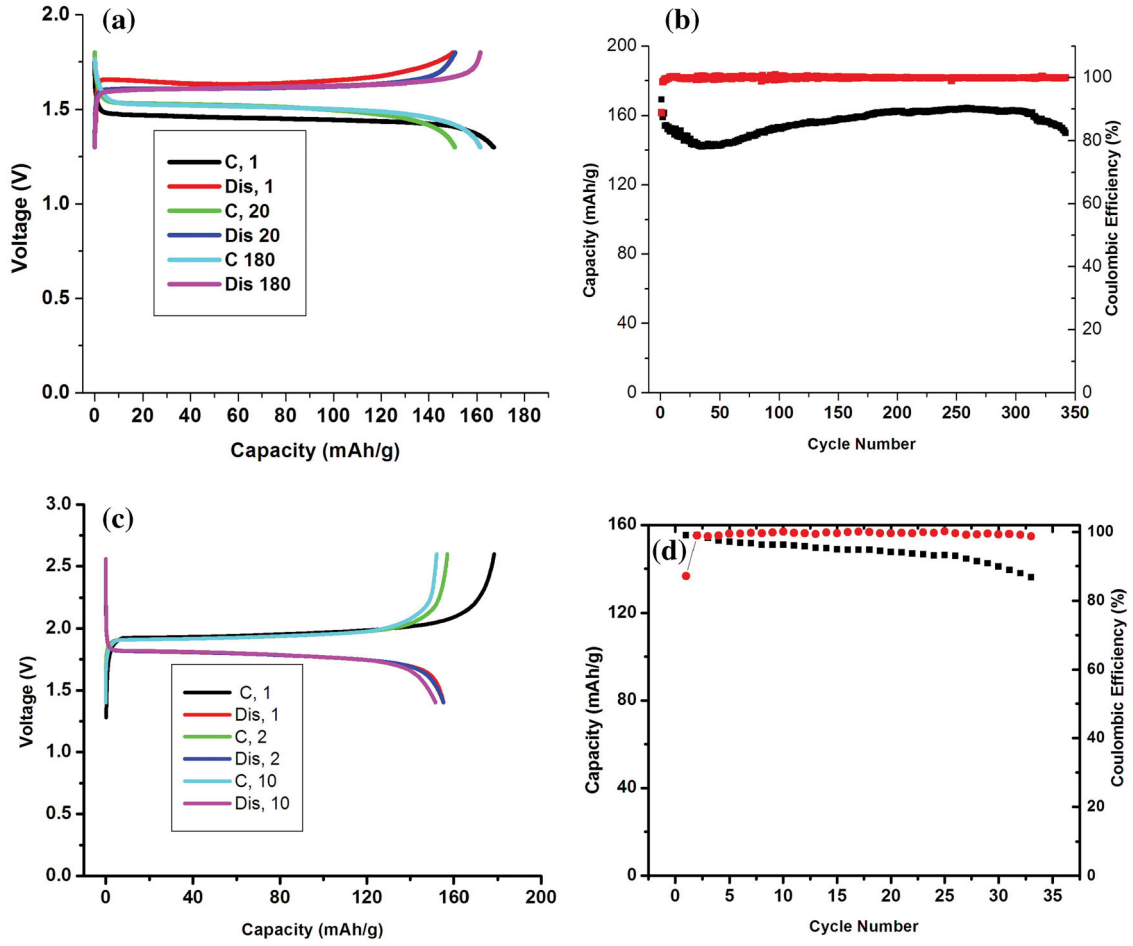

Figure 4. (a) Charge and discharge voltage profile of a half cell of 3D $Li_4Ti_5O_{12}$ vs. Li metal as the counter electrode. 1, 20 and 180 indicate different cycle numbers. (b) Discharge capacity and Coulombic efficiency vs. cycle number for a half cell of 3D $Li_4Ti_5O_{12}$ vs. Li metal as counter electrode between 1.3–1.8 V. (c) Voltage profile of a full cell, using 3D $Li_4Ti_5O_{12}$ as the anode and $LiFePO_4$ as the cathode. 1, 2 and 10 indicate different cycle numbers. (d) Discharge capacity and Coulombic efficiency vs. cycle number for full cells in (c).

Experimental Section

Current Collector Fabrication: CNT ink in water was made by dispersing purified CNTs in water with SDBS surfactant. The concentration of CNT is 1.6 mg/mL and of SDBS is 10 mg/mL. After bath sonication for 5 min, the CNT dispersion was probe sonicated for 30 min at 200 W (VC 505; Sonics) to form a black, well-dispersed CNT ink. A piece of textile made of randomly intertwined polyester fibers (Cloud 9 dream fleece, Wal-Mart Inc) was then dipped the CNT ink and taken out to dry on a metal mesh for 10 minutes in a vacuum oven at 100 °C. The polyester fibers have diameters ~20 µm. The dried textile is washed in DI water until no bubbles are observed. The final, black textile is highly conductive, which was referred to as a 3D current collector due to its large pores.

Filling Battery Materials into Porous Textile Conductor: Slurries of battery materials, $Li_4Ti_5O_{12}$ (Süd Chemie) and $LiFePO_4$ (Aleees LLC), are prepared by mixing 70 wt% active materials, 20 wt% Super P Carbon, and 10 wt% polyvinylidene fluoride (PVDF) binder in N-methyl-2-pyrrolidone (NMP) as the solvent. Typically, the mass for $Li_4Ti_5O_{12}$ or $LiFePO_4$ is 0.5 g and the volume for NMP is 3 mL. The slurries are well stirred overnight before use. The conductive textile is immersed into the batteries slurries and taken out after one minute soaking. The conductive textile with slurry coating is dried for overnight in a vacuum oven at 100 °C to completely remove the solvent. Finally, a solid, flexible conductive textile filled with battery electrode materials is ready for battery testing. The energy textile is bendable and can be easily cut into different shapes without delamination of the battery electrode materials from the conductive polyester fibers.

Fabrication and Testing of Three-Electrode Cells: The pouch was purchased by Aldrich. The reference electrode was based on $LiFePO_4$ on Al mesh, which was discharged at half of its capacity. In this way a stable electrode is obtained, with a very reproducible potential (U_{ref} = 3.428 V vs. Li/Li^+). Metallic lithium was used as the counter electrode. A 1 M solution of $LiPF_6$ in EC/DEC (1:1 vol/vol; Ferro) was used as the electrolyte. The charge-discharge cycles were performed at 10 mA g^{-1} at room temperature. EIS was performed at open circuit voltage, in the galvanostatic mode, using a current density of 500 µA/g, frequency range 100 kHz–0.1 Hz. The devices were assembled in an argon-filled glovebox with oxygen and water contents below 1 and 0.1 ppm, respectively. The Li-ion battery tests were performed by a Bio-Logic VMP3 battery tester. $LiFePO_4$ embedded in 3D textile current collectors was used as the working electrode.

Fabrication and Testing of Two-Electrode Cells: The parts for coin cell assembly were purchased from MTI Corporation, CA, USA. A 1M solution of $LiPF_6$ in EC/DEC (1:1 vol/vol; Ferro) was used as the electrolyte. The charge-discharge cycles were performed at different rates at room temperature. The devices were assembled in an argon-filled glovebox with oxygen and water contents below 1 and 0.1 ppm, respectively. The Li-ion battery tests were performed by either a Bio-Logic VMP3 battery

tester or an MTI battery analyzer. For half cells, Li-metal is used as the counter electrode, i.e., anode. In the full cells, $Li_4Ti_5O_{12}$ embedded in the conductive 3D textile current collector is used as the anode and $LiFePO_4$ embedded in the 3D textile current collector as the cathode.

Self-Discharge Test: The full cell was assembled and first cycled between 1.4–2.6 V for five cycles before the self-discharge test. The batteries were charged to 2.6 V and then disconnected for a certain period of time before discharge full down to 1.4 V. The disconnected periods tested were 0.1, 2, 10, 20, 100 and 200 hours. The self-discharge is plotted vs. disconnected periods in a log scale.

Acknowledgements

We acknowledge support from the King Abdullah University of Science and Technology (KAUST) Investigator Award (No. KUS-l1-001-12). J. McDonough acknowledges the support of the National Defense Science and Engineering and National Science Foundation Graduate Research Fellowships.

Received: May 19, 2011
Published online:

[1] J. M. Tarascon, M. Armand, *Nature* **2001**, *414*, 359.
[2] T. B. R. David Linden, *Handbook of Batteries*, McGraw-Hill Professional, **2001**.
[3] R. Moshtev, B. Johnson, *J. Power Sources* **2000**, *91*, 86.
[4] D. Aurbach, B. Markovsky, A. Rodkin, M. Cojocaru, E. Levi, H. J. Kim, *Electrochim. Acta* **2002**, *47*, 1899.
[5] J. W. Long, B. Dunn, D. R. Rolison, H. S. White, *Chem. Rev.* **2004**, *104*, 4463.
[6] L. B. Hu, J. W. Choi, Y. Yang, S. Jeong, F. La Mantia, L. F. Cui, Y. Cui, *Proc. Nat. Acad.Sci. USA* **2009**, *106*, 21490.
[7] L. B. Hu, M. Pasta, F. La Mantia, L. F. Cui, S. Jeong, H. D. Deshazer, J. W. Choi, S. M. Han, Y. Cui, *Nano Lett.* **2010**, *10*, 708.
[8] P. C. Chen, H. T. Chen, J. Qiu, C. W. Zhou, *Nano Res.* *3*, 594–603.
[9] A. Laforgue, *J. Power Sources 196*, 559.
[10] R. Bhattacharya, M. M. de Kok, J. Zhou, *Appl. Phys. Lett.* **2009**, *95*, 223305.
[11] S. Trohalaki, *MRS Bull.* **2006**, *35*, 175.
[12] D. Karst, Y. Q. Yang, *AATCC Review* **2006**, *6*, 44.
[13] A. P. S. Sawhney, B. Condon, K. V. Singh, S. S. Pang, G. Li, D. Hui, *Textile Res. J.* **2008**, *78*, 731.
[14] B. S. Shim, W. Chen, C. Doty, C. L. Xu, N. A. Kotov, *Nano Lett.* **2008**, *8*, 4151.
[15] M. F. Islam, E. Rojas, D. M. Bergey, A. T. Johnson, A. G. Yodh, *Nano Lett.* **2003**, *3*, 269.
[16] A. K. Mohanty, M. Misra, G. Hinrichsen, *Macromol. Mater. Eng.* **2000**, *276*, 1.
[17] D. N. Saheb, J. P. Jog, *Adv. Polym. Technol.* **1999**, *18*, 351.
[18] S. H. Ng, J. Wang, Z. P. Guo, G. X. Wang, H. K. Liu, *Electrochim. Acta* **2005**, *51*, 23.
[19] N. See-How, F. La Mantia, P. Novak, *Angew. Chem. Int. Ed.* **2009**, 48, 528.
[20] M. E. O. B. Tribollet, *Electrochemical Impedance Spectroscopy*, Wiley, **2008**.
[21] F. La Mantia, J. Vetter, P. Novak, *Electrochimica Acta* **2008**, *53*, 4109.
[22] S. Devan, V. R. Subramanian, R. E. White, *J. Electrochem. Soc.* **2004**, *151*, A905.
[23] K. Zaghib, M. Simoneau, M. Armand, M. Gauthier, *J. Power Sources* **1999**, *81*, 300.